PROCEEDINGS OF SCIENCE

First measurements of deuteron production spectra in *p+p* collisions at beam momentum of 158 GeV/c at the NA61/SHINE spectrometer at the CERN SPS

Anirvan Shukla[a,*] **on behalf of the NA61/SHINE Collaboration**

[a] *University of Hawai'i at Mānoa, Honolulu, Hawai'i, USA*

E-mail: anirvan@hawaii.edu

The NA61/SHINE spectrometer at the CERN Super Proton Synchrotron (SPS) scans particle production in collisions of nuclei with various sizes at a set of energies covering the SPS energy range towards various physics goals.
This paper presents the first differential production measurements of deuterons at energies relevant for cosmic-ray studies, produced in inelastic *p+p* interactions at incident projectile momentum of 158 GeV/c ($\sqrt{s}$ = 17.3 GeV). The double-differential spectra are presented as functions of rapidity and transverse momentum and are compared to predictions of the thermal and coalescence models. These measurements are essential for improving our understanding of cosmic (anti)nuclei production, as detecting cosmic antinuclei can be a breakthrough approach to identifying dark matter. The primary source of cosmic antinuclei background is interactions between cosmic-ray protons and interstellar hydrogen gas. Gaining a deeper insight into the deuteron production mechanism in *p+p* interactions is an essential first step in modeling cosmic antinuclei production.

39th International Cosmic Ray Conference (ICRC2025)
15–24 July 2025
Geneva, Switzerland

*Speaker

PoS(ICRC2025)397

1. Introduction

Detecting cosmic antinuclei can be a breakthrough approach for identifying dark matter [1]. The primary source of cosmic antinuclei background is interactions between cosmic-ray protons and interstellar hydrogen gas. Gaining a deeper insight into deuteron production in p+p interactions is an essential first step in modeling these astrophysical processes [2, 3]. The two most prevalent formation models, the thermal and coalescence models, are based on different underlying physics. A better understanding of (anti)nuclei production mechanisms is needed, which drives the effort to analyze high-statistics data sets from fixed-target experiments [4].

Unlike antideuterons, cosmic-ray deuterons have been measured [5–7], and they are the most abundant secondary cosmic-ray species in the Galaxy. Cosmic-ray deuterons disintegrate during nuclear processes in star-forming regions. Therefore, unlike primary cosmic-ray particles like protons and helium, they are not anticipated to be accelerated in supernova remnants. Rather, deuteron formation in cosmic rays (CRs) is understood to be mainly because of CR interactions with the interstellar medium [7, 8]. Secondary cosmic-ray deuterons are produced chiefly by two processes: fragmentation of CR nuclei such as ^{3}He and ^{4}He on interstellar hydrogen and helium, and the low-energy resonance reaction $p + p \rightarrow d + \pi^+$. Fragmentation is the main source of CR deuterons, because the resonance production channel is only possible at very low collision energies below 1 GeV [2, 9]. In addition to these two mechanisms, deuteron production in p+p and p+A interactions has also been measured in ground-based collider experiments, for example via:

$$p + p \rightarrow p + \overline{n} + d. \tag{1}$$

Of the three deuteron-producing mechanisms described above, the third mechanism (Eq. 1) is the only process that also allows the formation of secondary cosmic-ray antinuclei such as antideuterons and antihelium. (Anti)nuclei production via this mechanism can be modeled using the coalescence model, in which free nucleons resulting from CR–ISM interactions may coalesce to form deuterons [2, 3]. It can also be modeled with the thermal model [10–13], as well as transport models such as AMPT [14–16]. Examining particle yield measurements in p+p interactions over a large phase space range enables discrimination between different models. However, existing p+p data in the momentum range relevant to cosmic antideuterons are limited and have significant uncertainties [1, 2].

Understanding deuteron production in p+p interactions at energies between 100–400 GeV/c is a necessary first step to understand how CR antinuclei are produced [2]. This will also help towards developing a quantum mechanical description of the (anti)nuclei formation process [17–21]. Apart from the importance of these new deuteron measurements for both nuclear physics and in the interpretation of cosmic-ray measurements, this analysis will also serve as the basis of future antideuteron measurements with ultra-high statistics at NA61/SHINE.

NA61/SHINE at the CERN Super Proton Synchrotron (SPS) performs systematic studies of hadron production in strong interactions to address open questions in cosmic-ray physics and in the exploration of the phase diagram of strongly interacting matter. Previous results [22] have been used in several cosmic-ray studies, highlighting their importance for interpreting cosmic-ray data [1–3, 23–26].

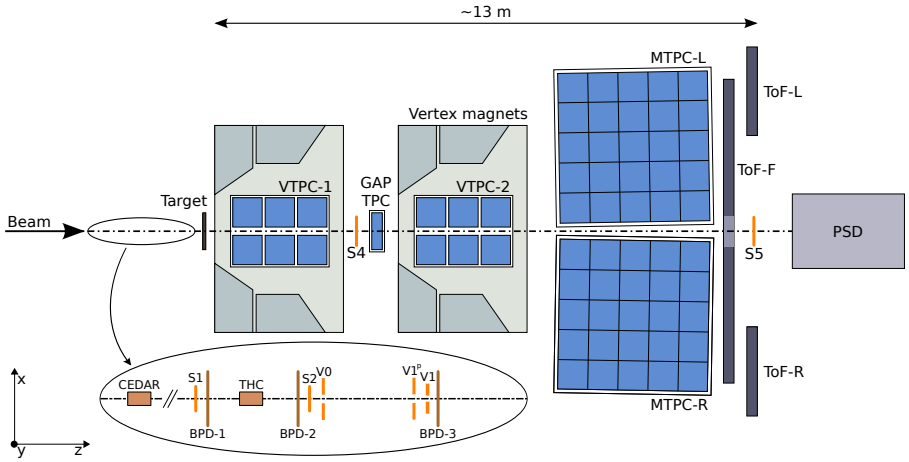

Figure 1: Schematic layout of the NA61/SHINE facility at the CERN SPS used for p+p data taking [29] (horizontal cut, not to scale). The beam instrumentation is sketched in the inset. The nominal beam direction is along the z axis. The magnetic field bends charged particle trajectories in the x-z plane. The electron drift direction in the TPCs is along the y (vertical) axis.

The NA49 experiment [27], the predecessor of NA61/SHINE at CERN SPS, analyzed Pb+Pb interactions at 158 GeV/c beam momentum. It was demonstrated that both deuterons and antideuterons can be identified in this experimental setup [28]. While measurements from heavy-ion collisions cannot be directly applied to p+p interactions due to the large difference in the system size [3], the NA49 analysis demonstrated the feasibility of a similar analysis of the high-statistics p+p data sets in NA61/SHINE, which has recorded more than 60 million p+p collisions at beam momentum of 158 GeV/c.

It is worth noting that deuteron production is quite rare in p+p interactions at SPS energies of ~100–400 GeV. For beam momentum p_{beam} = 158 GeV/c, the coalescence parametrization developed in Refs. [2, 3] predicted a per-event production probability of 0.0004, with an uncertainty band from 0.0002 to 0.0009. The total deuteron production cross section at kinetic energies around ~100 GeV was estimated in Ref. [2] to be close to 0.02 mb. To estimate the phase space acceptance for deuterons, about 2.7 trillion p+p interactions were simulated at p_{beam} = 158 GeV/c. Deuteron production in these interactions was simulated by applying the coalescence afterburner condition for seven different values of the coalescence momentum p_0 [2, 3].

The phase space accessible to deuterons coincides with peak deuteron production in the center-of-mass frame's backward hemisphere, but detector efficiency and acceptance limit identification to roughly 1–2 % of the total deuterons produced.

2. Experimental Setup

NA61/SHINE receives proton and ion beams from CERN SPS H2 beam line up to 158 A GeV/c, for a broad physics program [29, 30]. Dipole and quadrupole magnets guide the beam, and its position is monitored by scintillators S1/S2 and Beam Position Detectors (BPDs). Particle tracking and identification are provided by three Time Projection Chambers (TPCs): two Vertex TPCs (VTPC-1/2) inside superconducting magnets providing 9 Tm of bending power, a small GAP

Table 1: Summary of the recorded high-statistics p+p interactions at $p_{\text{beam}} = 158\,\text{GeV}/c$ in NA61/SHINE.

Year	p+p interactions recorded	Total selected events
2009	3.8 million	1.6 million
2010	43.1 million	25.6 million
2011	13.7 million	8.1 million
Total	60.6 million	35.3 million

TPC, and two large Main TPCs (MTPC-L/R). These are augmented by two downstream time-of-flight (ToF) detectors, ToF-L and ToF-R.

A minimum-bias trigger selects interactions in the liquid-hydrogen target (LHT) by requiring an incident beam proton in S1 and its disappearance downstream of the target in the S4 counter, suppressing elastic events [22]. Detailed detector and trigger descriptions are provided in Refs. [4, 22, 29].

3. Data Selection

This deuteron analysis is based on the p+p data sets collected at NA61/SHINE in 2009, 2010, and 2011. A total of more than 60 million p+p collisions at beam momentum of 158 GeV/c were recorded, which yielded more than 750 million reconstructed particle tracks.

The overall analysis procedure consists of the following steps:

1. Event and track selection.
2. Calculation of raw (i.e., uncorrected for biases) particle count distributions of identified charged hadrons.
3. Applying data-derived and simulation-based corrections to the raw counts.
4. Calculation of the corrected particle spectra.
5. Estimation of statistical and systematic uncertainties.

Events with inelastic p+p interactions were selected based on five key criteria. First, the presence of off-time beam particles was rejected by identifying multiple beam signals within $\pm 2\,\mu$s around the primary trigger particle. Second, the beam proton trajectory was validated by ensuring sufficient signals in the Beam Position Detectors (BPDs), particularly BPD3 which is nearest to the target. Third, each event was required to contain at least one track originating from the reconstructed main p+p interaction vertex. Fourth, the z-position of the main vertex was constrained to lie within $\pm 20\,$cm of the target center. Finally, events were rejected if they contained only one positively charged track with momentum matching that of the incident beam, thus removing elastic scattering candidates. These combined selection steps ensured a consistent dataset of purely inelastic p+p interactions for both data and simulation analyses.

Reconstructed particle tracks were selected to ensure only primary charged hadrons were retained and to minimize contamination from off-time interactions, weak decays, and secondary interactions. First, each track had to originate from the main interaction vertex, with a convergent momentum fit. Next, track were required to satisfy the condition $p_{\text{lab},x}/q > 0$, where $p_{\text{lab},x}$ is the x-component of the total momentum in the laboratory frame and q is the particle's charge. This

positive-rigidity cut preferentially retains tracks with smaller uncertainties in the track fit and cluster reconstruction [31]. Tracks also needed at least 30 reconstructed clusters, including a minimum of 15 clusters in the Vertex TPCs (or at least 4 in the Gap TPC), and a similarly stringent requirement for $\mathrm{d}E/\mathrm{d}x$ clusters. Finally, the distance between the main vertex and the track extrapolation in the transverse plane (impact parameter) had to be within 4 cm horizontally and 2 cm vertically. These criteria ensured precise momentum measurement and reliable track identification of primary charged hadrons.

4. Data Analysis

After the application of event and track quality cuts, about 35 million collision events containing about 60 million particle tracks were selected for analysis. The recorded event statistics are summarized in Table 1.

4.1 Particle Identification Based on Time of Flight and Energy Loss Measurement

Deuterons were identified with the $tof - \mathrm{d}E/\mathrm{d}x$ method, which combines the energy loss measurements ($\mathrm{d}E/\mathrm{d}x$) in the TPCs with the m^2 measurements from the ToF detectors. A clean deuteron signal was extracted in regions of large negative rapidity, in the backward hemisphere of the center-of-mass frame (approximately $y = -1$).

After the standard event and track selection cuts described in Sec. 3, ToF–specific criteria ensured precise track–pixel matching and noise suppression [4, 32]. These additional cuts are:

1. The hit in the ToF scintillator pixel must be associated with only one reconstructed TPC track.
2. The ToF hit pixel must coincide with the extrapolated pixel where the MTPC track, linearly extrapolated from its last ten clusters in the x–z and y–z planes, intersects the ToF wall.
3. The hit pixel must have corresponding ADC and TDC measurements [33].
4. The last point measured on the MTPC track was required to be in the last two padrows of the MTPC to ensure good matching between the TPC tracks and ToF walls.
5. Track residual distance was calculated between the reconstructed global particle trajectory and the last point measured on the track in the MTPC, and it was required to be less than 2 cm.
6. Finally, the minimum overall efficiency of a ToF pixel used in these measurements was set to 50%. Pixel with hit efficiencies less than 50% were categorized as dead, and were not used for measurements.

Applying these conditions provided reliable extrapolation of the MTPC trajectories toward the ToF detectors, and helped in reducing noise in the selected tracks.

4.2 Deuteron Identification using m^2 Distributions

The standard particle identification (PID) technique in the $tof - \mathrm{d}E/\mathrm{d}x$ analysis relies on two-dimensional fits performed in the m^2–$\mathrm{d}E/\mathrm{d}x$ plane and was successful in identifying charged hadrons in p+p and Ar+Sc data sets [22, 34]. However, this technique is unable to estimate the deuterons under the proton tail.

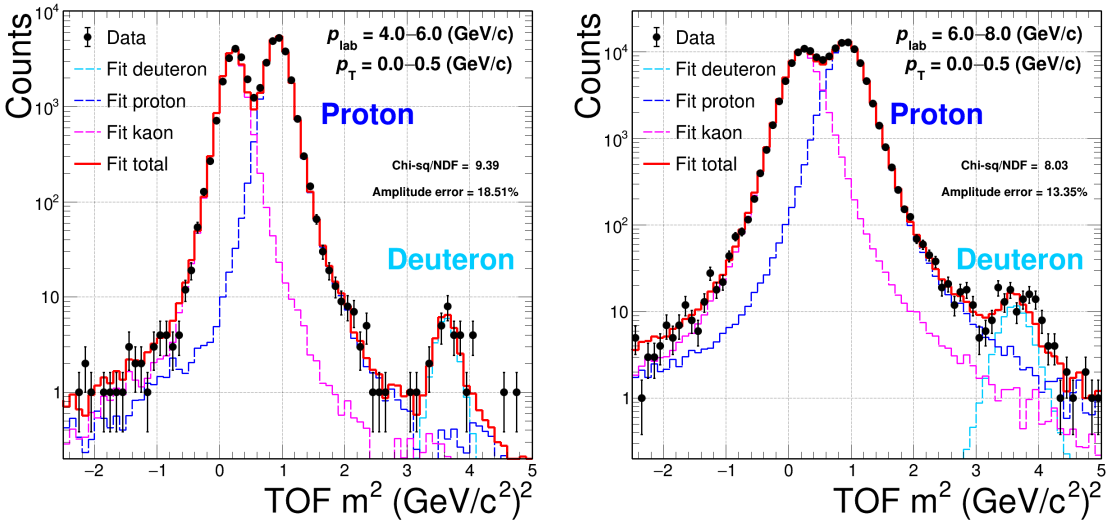

Figure 2: Two example phase space bins with data-driven pion-mass templates to fit the kaon, proton and deuteron peaks.

Therefore, a new data-driven template fitting method was developed for particle identification [35]. For each total momentum and transverse momentum (p_{tot}, p_{T}) bin, pions and positrons were separated from the other particles using the $\mathrm{d}E/\mathrm{d}x$ information by applying cuts on the $\mathrm{d}E/\mathrm{d}x$–momentum plane. As the mass distributions for kaons, protons, and deuterons overlap, the pion mass distribution was modified for detector resolution effects and the kaon, proton, and deuteron mass, respectively. These three modified mass templates served as the input for the combined one-dimensional m^2 template fit of the higher-mass $Z = 1$-particle mass spectra.

Figure 2 shows two example (p_{tot}, p_{T}) bins with a clear deuteron peak. It also illustrates the importance of realistically estimating the proton tail in the deuteron mass region. The kaon, proton, and deuteron yield extraction is based on the probability method (Sec. 4.3).

4.3 Deuteron Yields with the Probability Method

The estimation of the deuteron yields was done using a modified probability method [4, 22, 34]. In this method, the fits of the m^2 distributions were used to compute the probabilities P_i for a track being a given particle type $i = p, K, d$. After obtaining the m^2 fits described above, these probabilities can be calculated as:

$$P_i(m^2, p_{\text{lab}}, p_{\text{T}}) = \frac{\rho_i(m^2, p_{\text{lab}}, p_{\text{T}})}{\sum\limits_{i=p,K,d} \rho_i(m^2, p_{\text{lab}}, p_{\text{T}})}, \tag{2}$$

where ρ_i is the value of the fitted function for particle-type i in a given (p_{lab}, p_{T}) bin, evaluated at the m^2 of the particle. The denominator represents the total fit value for that bin at the particle's m^2. It is assumed that pions and positrons were perfectly identified using the cuts on $\mathrm{d}E/\mathrm{d}x$–momentum plane. The probability method assigned each track probabilities of being a pion, positron, kaon, proton, or deuteron.

The probabilities are either 0 or 1 if the particle was identified as a pion or an electron. Because of the overlapping m^2 distributions, the calculated particle probability values for kaons, protons

and deuterons range between 0 and 1. Using this method, the fits performed in $(p_{\text{tot}}, p_{\text{T}})$ bins were used to get count distributions in (y, p_{T}) bins. The total number of raw (i.e., uncorrected) identified particles n^{raw} of particle-type i in a given kinematic bin (e.g., (y, p_{T})) is given by [36]:

$$n^{\text{raw}}_{i=\pi,K,p,d} = \sum_{j=1}^{N_{\text{trk}}} P_i, \tag{3}$$

where P_i is the probability of particle type i given by Eq. 2, and j is the index to sum over all N_{trk} weights in the given kinematic bin.

Approximately 10% of the statistics were recorded with the liquid-hydrogen target removed to quantify off-target backgrounds. The target-removed sample was scaled by the ratio of events with fitted vertices in the range $-400 < z < -200$ cm between target-inserted and target-removed runs, and its yield was then subtracted for each bin of total momentum and transverse momentum. After background subtraction, the final particle counts were measured in two-dimensional bins of rapidity (y) and transverse momentum (p_{T}). About 200 deuteron tracks could be identified. The particle rapidity was calculated in the collision center-of-mass frame. The bin size was chosen taking into account the statistical uncertainties and the resolution of the momentum reconstruction, to reduce the effect of bin-to-bin migration to less than 1% [37]. To finalize the particle spectra, (y, p_{T})-dependent correction factors for detector geometry and ToF-related efficiencies were calculated using Monte Carlo simulations, and applied to correct the normalized raw count distributions.

4.4 Estimation of Systematic and Statistical Uncertainties

A preliminary evaluation of both statistical and systematic uncertainties was performed for the preliminary deuteron spectra.

Statistical uncertainties were obtained by treating the raw, background-subtracted total deuteron counts in each (y, p_{T}) bin as independent Poisson variables. The error was subsequently propagated through the spectra calculation. The resulting relative statistical errors are large and range from approximately 30% to 60%, reflecting the limited statistics available in these kinematic regions.

The dominant sources of systematic uncertainties are those associated with the one-dimensional m^2 fits and the modeling of the proton tail under the deuteron peak. The deuteron signal sits on a broad background arising primarily from the high-mass tail of the proton m^2 distribution. A data-driven template fit is employed to model this tail. The template shape parameters are varied within the detector resolution envelope, and the deuteron yield is re–extracted for each variation. The maximum spread of the refitted yields, about ±20%, is assigned as the systematic uncertainty associated with the background proton subtraction.

The baseline analysis employs fixed-width bins of $\Delta p_{\text{lab}} = 2$ GeV/c and $\Delta p_{\text{T}} = 0.5$ GeV/c to perform the m^2 fits. Ten alternative grids are formed by halving one or both of these widths. The root-mean-square (RMS) spread of the resulting deuteron yields is 15%, which is taken as the systematic uncertainty due to the choice of phase-space slicing. The two leading systematic contributions are uncorrelated and are therefore combined in quadrature:

$$\Delta_{\text{syst}} = \sqrt{(20\%)^2 + (15\%)^2} \approx 25\%.$$

This bin-independent envelope is quoted alongside the Poisson statistical bars for every spectra point.

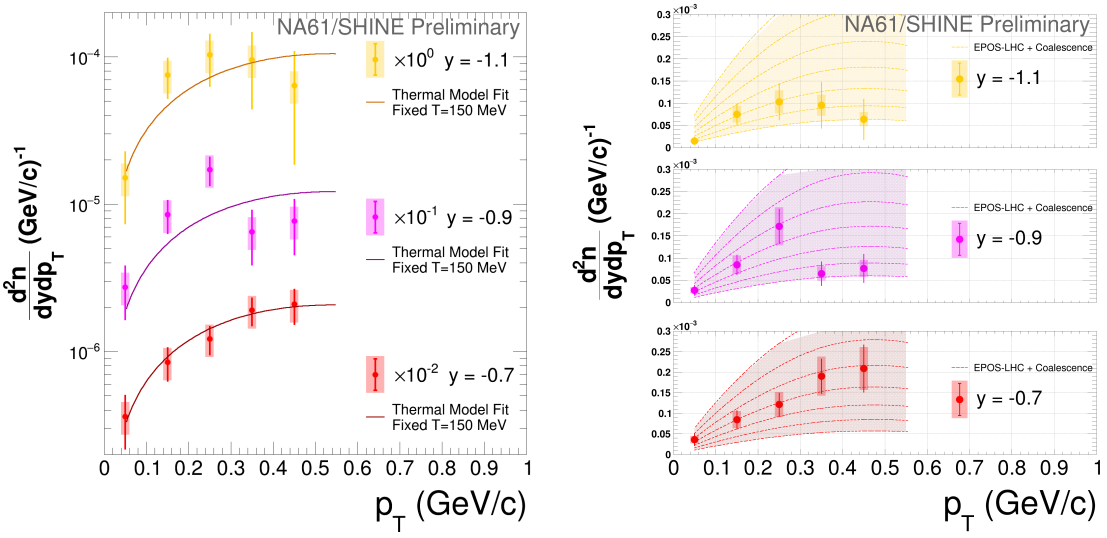

Figure 3: Left: Preliminary transverse momentum spectra in rapidity slices for deuterons in inelastic p+p interactions at 158 GeV/c. Solid lines show the overlaid two-parameter thermal model with the shape parameter fixed to T = 150 MeV (from Ref. [22]). Only the amplitude parameter was fitted to the data. Right: Preliminary deuteron transverse momentum spectra in rapidity slices compared to the coalescence model predictions from Refs. [2, 3].

4.5 Validation of Methods

The new techniques in this analysis were validated in two independent ways. First, in each (p_{tot}, p_{T}) bin, the fitted proton counts from the new fitting technique were compared to the fitted proton counts from the standard method of making two-dimensional fits. This ratio was found to be almost-exactly 1 in almost every (p_{tot}, p_{T}) bin, with a very small associated uncertainty. Second, the identified proton spectra from the new $tof - \mathrm{d}E/\mathrm{d}x$ technique were compared to the previously-published proton spectra for all available overlapping phase space bins. The comparison showed that the new proton spectra from the $tof - \mathrm{d}E/\mathrm{d}x$ analysis overlapped with published measurements within the uncertainty bands [32]. Both these checks were used to validate the new technique.

5. Results

The preliminary transverse momentum spectra in rapidity slices for deuterons produced in inelastic p+p interactions at 158 GeV/c are presented in Fig. 3. Figure 3 (left) shows an overlay of the thermal model (solid lines) with the data. The thermal model is characterized by two parameters: the temperature T, which defines the shape of the distribution, and an amplitude factor. For illustrative purposes, the temperature has been set to T = 150 MeV, consistent with measurements from Ref. [22]), and only the amplitude was fitted to the data. The overlay demonstrates the agreement between the data and the thermal model. Figure 3 (right) presents a comparison with the predicted spectra band from the coalescence model developed in Refs. [2, 3]. Both the thermal and coalescence models show good agreement with the experimental data within the current level of uncertainties.

Detailed cross-checks have been developed to account for the deuterons produced by interaction of secondary protons inside the detector. The contribution of secondary proton interactions with the right target holder window was estimated to be negligible [4]. The contribution of secondary protons reinteractions within the liquid hydrogen of the target was estimated to be less than ~2% [4]. Further studies to estimate the secondary deuteron background using Geant4 simulation are ongoing.

6. Summary and Outlook

Following the success of the first deuteron yield measurement in the p+p 158 GeV/c data set using the tof–dE/dx analysis presented in this work, the next step was to look at the negatively charged tracks. About 5×10^4 antiprotons were identified by the preliminary application of the tof − dE/dx analysis framework developed in the previous sections to analyze negatively charged tracks. For the same collision system, antideuteron production is about ~1000 times smaller than antiproton production [3]. Applying this to all measurable phase space bins leads to an expectation of about 50 antideuterons in the existing p+p 158 GeV/c data sets. A few such p+p collision events with an antideuteron candidate, which pass all quality and selection cuts, have been identified.

The identification of antideuteron candidates in existing data motivates continued measurements with the upgraded NA61/SHINE detector. During the CERN Long Shutdown 2, new TPC backend electronics resulted in a reduction of noise as well as improvement in the dE/dx resolution. Upgraded TPC readout electronics increased the data-taking rate to 1.6 kHz (~20× faster). New ToF detector with better timing resolution have also been installed [38, 39].

In October 2025, the CERN SPS accelerator will deliver an unprecedented 600 million p+p collisions at 300 GeV/c to NA61/SHINE, corresponding to a center-of-mass energy of approximately 24 GeV. Collisions at this energy are particularly relevant for studying the production of secondary antinuclei in cosmic rays. This 10× larger dataset will not only complement existing measurements but also offer a 3× improvement in statistical precision. With the increased energy and number of events, an estimated 3000 deuterons and 100 antideuterons could potentially be identified [21]. The anticipated reduction in systematic and statistical uncertainties will be instrumental in building and validating new, updated models for the production of astrophysical antideuterons. This could be an essential breakthrough to understand the nature of dark matter.

PoS(ICRC2025)397

Acknowledgments

We would like to thank the CERN EP, BE, HSE and EN Departments for the strong support of NA61/SHINE. This work was supported by the Hungarian Scientific Research Fund (grant NKFIH 138136/137812/138152 and TKP2021-NKTA-64), the Polish Ministry of Science and Higher Education (DIR/WK/2016/2017/10-1, WUT ID-UB), the National Science Centre Poland (grants 2014/14/E/ST2/00018, 2016/21/D/ST2/01983, 2017/25/N/ST2/02575, 2018/29/N/ST2/02595, 2018/30/A/ST2/00226, 2018/31/G/ST2/03910, 2020/39/O/ST2/00277), the Norwegian Financial Mechanism 2014–2021 (grant 2019/34/H/ST2/00585), the Polish Minister of Education and Science (contract No. 2021/WK/10), the European Union's Horizon 2020 research and innovation programme under grant agreement No. 871072, the Ministry of Education, Culture, Sports, Science and Technology, Japan, Grant-in-Aid for Scientific Research (grants 18071005, 19034011, 19740162, 20740160 and 20039012,22H04943), the German Research Foundation DFG (grants GA 1480/8-1 and project 426579465), the Bulgarian Ministry of Education and Science within the National Roadmap for Research Infrastructures 2020–2027, contract No. D01-374/18.12.2020, Serbian Ministry of Science, Technological Development and Innovation (grant OI171002), Swiss Nationalfonds Foundation (grant 200020117913/1), ETH Research Grant TH-01 07-3, National Science Foundation grants PHY-2013228 and PHY-2411633 and the Fermi National Accelerator Laboratory (Fermilab), a U.S. Department of Energy, Office of Science, HEP User Facility managed by Fermi Research Alliance, LLC (FRA), acting under Contract No. DE-AC02-07CH11359 and the IN2P3-CNRS (France).

Bibliography

[1] P. von Doetinchem et al. *Journal of Cosmology and Astroparticle Physics* **2020** (2020) 035–035.

[2] D.-M. Gomez-Coral *et al.* *Physical Review D* **98** (2018) 023012.

[3] A. Shukla, A. Datta, P. von Doetinchem, D.-M. Gomez-Coral, and C. Kanitz *Phys. Rev. D* **102** (2020) 063004.

[4] A. Shukla "Light nuclei and antinuclei production in proton-proton interactions," PhD thesis CERN-THESIS-2023-051, University of Hawaii at Manoa, 2023. https://cds.cern.ch/record/2859334.

[5] R. Sina, V. Ptuskin, and E. S. Seo *International Cosmic Ray Conference* **4** (2003) 1973.

[6] N. Tomassetti and J. Feng *The Astrophysical Journal* **835** (2017) L26.

[7] M. A. et al., [AMS Collab.] *Phys. Rev. Lett.* **132** (2024) 261001. https://link.aps.org/doi/10.1103/PhysRevLett.132.261001.

[8] D. M. Gomez-Coral, C. Gerrity, R. Munini, and P. von Doetinchem *Phys. Rev. D* **107** (2023) 123008. https://link.aps.org/doi/10.1103/PhysRevD.107.123008.

[9] J. P. Meyer *Astron. Astrophys. Suppl. Ser.* **7** (1972) 417.

[10] F. Becattini and U. W. Heinz *Zeitschrift für Physik C Particles and Fields C* **76** (1997) 269–286. [Erratum: Z. Phys.C76,578(1997)].

[11] A. Andronic, P. Braun-Munzinger, J. Stachel, and H. Stöcker *Physics Letters B* **697** (2011) 203 – 207.

[12] J. Cleymans, S. Kabana, I. Kraus, H. Oeschler, K. Redlich, and N. Sharma *Physical Review C* **84** (2011) 054916.

[13] F. Bellini and A. P. Kalweit *Physical Review C* **99** (2019) 054905.

[14] Z.-W. Lin, C. M. Ko, B.-A. Li, B. Zhang, and S. Pal *Phys. Rev. C* **72** (2005) 064901. https://link.aps.org/doi/10.1103/PhysRevC.72.064901.

[15] F.-X. Liu, Z.-L. She, H.-G. Xu, D.-M. Zhou, G. Chen, and B.-H. Sa *Scientific Reports* **12** (2022) 1772.

[16] T. Shao, J. Chen, Y.-G. Ma, and Z. Xu *Physical Review C* **105** (2022) 065801.

[17] R. Scheibl and U. W. Heinz *Physical Review C* **59** (1999) 1585–1602.

[18] K. B. et al. *Physical Review D* **96** (2017) 103021.

[19] M. Kachelrieß, S. Ostapchenko, and J. Tjemsland *European Physical Journal A* **56** (2020) 4.

[20] M. Kachelrieß, S. Ostapchenko, and J. Tjemsland *The European Physical Journal A* **57** (2021) 1434–601X. https://doi.org/10.1140%2Fepja%2Fs10050-021-00469-w.

[21] P. von Doetinchem, [NA61/SHINE Collab.] tech. rep., CERN, Geneva, 2024.

[22] A. Aduszkiewicz *et al.* *European Physical Journal C* **77** (2017) 671.

[23] M. Korsmeier, F. Donato, and M. Di Mauro *Physical Review D* **97** (2018) 103019.

[24] A. Cuoco, J. Heisig, L. Klamt, M. Korsmeier, and M. Krämer *Physical Review D* **99** (2019) 103014.

[25] M. K. et al. *Computer Physics Communications* **245** (2019) 106846.

[26] M. Boudaud, Y. Génolini, L. Derome, J. Lavalle, D. Maurin, P. Salati, and P. D. Serpico *Phys. Rev. Res.* **2** (2020) 023022.

[27] S. Afanasiev *et al.*, [NA49 Collab.] *Nucl. Instrum. Meth. A* **430** (1999) 210–244.

[28] T. A. et al. *Physical Review C* **85** (2012) 044913.

[29] N. Abgrall *et al.*, [NA61/SHINE Collab.] *JINST* **9** (2014) P06005.

[30] H. Adhikary *et al.*, [NA61/SHINE Collab.] *Phys. Rev. D* **107** (2023) 062004.

[31] P. Podlaski, *Study of charged hadron production with tof-dE/dx identification method in central Ar+Sc collisions in NA61/SHINE experiment at CERN.* PhD thesis, Warsaw University, 2021. https://cds.cern.ch/record/2799198. Figure 5.7.

[32] S. Kowalski and E. Zimmerman, [NA61/SHINE Collab.] tech. rep., CERN, Geneva, 2024.

[33] Podlaski, Piotr "Study of charged hadron production with tof-dE/dx identification method in central Ar+Sc collisions in NA61/SHINE experiment at CERN., Section 5.3.2 pp 51-53," PhD thesis CERN-THESIS-2021-250, Warsaw University, 2021. https://cds.cern.ch/record/2799198.

[34] H. Adhikary *et al. The European Physical Journal C* **84** (2024) 416. http://dx.doi.org/10.1140/epjc/s10052-024-12602-2.

[35] K. Grebieszkow, M. Mackowiak-Pawlowska, and P. Von Doetinchem, [NA61/SHINE Collab.] tech. rep., CERN, Geneva, 2023.

[36] A. Rustamov and M. Gorenstein *Phys.Rev.* **C86** (2012) 044906.

[37] N. Abgrall *et al.*, [NA61/SHINE Collab.] *Eur.Phys.J.* **C74** (2014) 2794.

[38] M. Gazdzicki, [NA61/SHINE Collab.] tech. rep., CERN, Geneva, 2019.

[39] A. Acharya *et al.*, [NA61/SHINE Collab.] Tech. Rep. CERN-SPSC-2020-023, SPSC-SR-278, CERN, Geneva, 2020.

PoS(ICRC2025)397

The NA61/SHINE Collaboration

H. Adhikary [11], P. Adrich [13], K.K. Allison [24], N. Amin [4], E.V. Andronov [20], I.-C. Arsene [10], M. Bajda [14], Y. Balkova [16], D. Battaglia [23], A. Bazgir [11], J. Bennemann [4], S. Bhosale [12], M. Bielewicz [13], A. Blondel [3], M. Bogomilov [2], Y. Bondar [11], A. Bravar [27], W. Bryliński [19], J. Brzychczyk [14], M. Buryakov [20], A.F. Camino [26], M. Ćirković [21], M. Csanád [6], J. Cybowska [19], T. Czopowicz [11], C. Dalmazzone [3], N. Davis [12], A. Dmitriev [20], P. von Doetinchem [25], W. Dominik [17], J. Dumarchez [3], R. Engel [4], G.A. Feofilov [20], L. Fields [23], Z. Fodor [5,18], M. Friend [7], M. Gaździcki [11], K.E. Gollwitzer [22], O. Golosov [20], V. Golovatyuk [20], M. Golubeva [20], K. Grebieszkow [19], F. Guber [20], P.G. Hurh [22], S. Ilieva [2], A. Ivashkin [20], A. Izvestnyy [20], N. Karpushkin [20], M. Kiełbowicz [12], V.A. Kireyeu [20], R. Kolesnikov [20], D. Kolev [2], Y. Koshio [8], S. Kowalski [16], B. Kozłowski [19], A. Krasnoperov [20], W. Kucewicz [15], M. Kuchowicz [18], M. Kuich [17], A. Kurepin [20], A. László [5], M. Lewicki [12], G. Lykasov [20], J. Lyon [25], V.V. Lyubushkin [20], M. Maćkowiak-Pawłowska [19], A. Makhnev [20], B. Maksiak [13], A.I. Malakhov [20], A. Marcinek [12], A.D. Marino [24], H.-J. Mathes [4], T. Matulewicz [17], V. Matveev [20], G.L. Melkumov [20], A. Merzlaya [10], Ł. Mik [15], S. Morozov [20], Y. Nagai [6], T. Nakadaira [7], M. Naskręt [18], S. Nishimori [7], A. Olivier [23], V. Ozvenchuk [12], O. Panova [11], V. Paolone [26], O. Petukhov [20], I. Pidhurskyi [11], R. Płaneta [14], P. Podlaski [17], B.A. Popov [20,3], B. Pórfy [5,6], D.S. Prokhorova [20], D. Pszczel [13], S. Puławski [16], R. Renfordt [16], L. Ren [24], V.Z. Reyna Ortiz [11], D. Röhrich [9], E. Rondio [13], M. Roth [4], Ł. Rozpłochowski [12], B.T. Rumberger [24], M. Rumyantsev [20], A. Rustamov [1], M. Rybczynski [11], A. Rybicki [12], D. Rybka [13], K. Sakashita [7], K. Schmidt [16], A. Seryakov [20], P. Seyboth [11], U.A. Shah [11], Y. Shiraishi [8], A. Shukla [25], M. Słodkowski [19], P. Staszel [14], G. Stefanek [11], J. Stepaniak [13], F. Sutter [4], Ł. Świderski [13], J. Szewiński [13], R. Szukiewicz [18], A. Taranenko [20], A. Tefelska [19], D. Tefelski [19], V. Tereshchenko [20], R. Tsenov [2], L. Turko [18], T.S. Tveter [10], M. Unger [4], M. Urbaniak [16], D. Veberič [4], O. Vitiuk [18], V. Volkov [20], A. Wickremasinghe [22], K. Witek [15], K. Wójcik [16], O. Wyszyński [11], A. Zaitsev [20], E. Zherebtsova [18], E.D. Zimmerman [24], and A. Zviagina [20]

[1] National Nuclear Research Center, Baku, Azerbaijan
[2] Faculty of Physics, University of Sofia, Sofia, Bulgaria
[3] LPNHE, Sorbonne University, CNRS/IN2P3, Paris, France
[4] Karlsruhe Institute of Technology, Karlsruhe, Germany
[5] HUN-REN Wigner Research Centre for Physics, Budapest, Hungary
[6] Eötvös Loránd University, Budapest, Hungary
[7] Institute for Particle and Nuclear Studies, Tsukuba, Japan
[8] Okayama University, Japan
[9] University of Bergen, Bergen, Norway
[10] University of Oslo, Oslo, Norway
[11] Jan Kochanowski University, Kielce, Poland
[12] Institute of Nuclear Physics, Polish Academy of Sciences, Cracow, Poland

PoS(ICRC2025)397

[13] National Centre for Nuclear Research, Warsaw, Poland
[14] Jagiellonian University, Cracow, Poland
[15] AGH - University of Krakow, Poland
[16] University of Silesia, Katowice, Poland
[17] University of Warsaw, Warsaw, Poland
[18] University of Wrocław, Wrocław, Poland
[19] Warsaw University of Technology, Warsaw, Poland
[20] Affiliated with an institution covered by a cooperation agreement with CERN
[21] University of Belgrade, Belgrade, Serbia
[22] Fermilab, Batavia, USA
[23] University of Notre Dame, Notre Dame, USA
[24] University of Colorado, Boulder, USA
[25] University of Hawaii at Manoa, Honolulu, USA
[26] University of Pittsburgh, Pittsburgh, USA
[27] University of Geneva, Geneva, Switzerland[1]

[1] No longer affiliated with the NA61/SHINE collaboration